# Improved Turn-On Times of Light-Emitting Electrochemical Cells

Eli Zysman-Colman,[†] Jason D. Slinker,[‡] Jeffrey B. Parker,[‡] George G. Malliaras,*[,‡] and Stefan Bernhard*[,†]

*Department of Chemistry, Princeton University, Frick Lab, Princeton, New Jersey 08544, and Department of Materials Science and Engineering, Cornell University, Ithaca, New York 14850*

*Received May 17, 2007. Revised Manuscript Received October 4, 2007*

Electroluminescent devices from ionic transition metal complexes (iTMCs) are attractive candidates for display and lighting applications. A major limitation of application of iTMC devices is their turn-on times, which range from minutes to hours at 3 V. We report novel ruthenium and iridium complexes with pendant triethylammonium groups bonded to the ligands with methylene units of various lengths. These materials lead to devices with turn-on times at 3 V as short as 2.5 min for the iridium complexes and as low as 5 s for the ruthenium complexes.

## Introduction

Ionic transition metal complexes (iTMCs) are garnering increased attention as candidates for display and lighting applications.[1–24] The operational characteristics of light-emitting devices from iTMCs are dominated by the presence of mobile ions in the solid-state iTMC layer.[25] Namely, upon application of a bias, the counterions associated with the complexes redistribute in the vicinity of the electrodes. This charge redistribution produces high electric fields at the electrode interfaces and enhances injection of holes and electrons at the anode and cathode, respectively, resulting in efficient electroluminescence at low turn-on voltages (<3 V), even with air-stable electrodes.[26,27] Efficient devices can be made by lamination,[28] with important implications for reel-to-reel processing. Furthermore, iTMCs enable the fabrication of fault-tolerant, scalable illumination panels[5,26,29,30] with ac line power operational capability.[30] The current state-of-the-art devices that incorporate an iTMC layer reach an external quantum efficiency of ca. 10%,[10,11,31] with current efficiencies as high as 60 cd/A. Recently, a green-light-emitting DPEphos copper complex-based device was fabricated with an EQE of 16% (56 cd/A).[31]

In order for electroluminescent devices to be of practical application, their turn-on times (the time it takes to reach maximum emission once a dc bias has been applied) need to be less than a few milliseconds.[32] Turn-on times are dependent upon counterion mobility within the iTMC film

* Corresponding author. E-mail: bern@Princeton.edu; ggm1@cornell.edu.
[†] Princeton University.
[‡] Cornell University.

(1) Baldo, M. A.; Lamansky, S.; Burrows, P. E.; Thompson, M. E.; Forrest, S. R. *Appl. Phys. Lett.* **1999**, *75*, 4.
(2) Nazeeruddin, M. K.; Wegh, R. T.; Zhou, Z.; Klein, C.; Wang, Q.; DeAngelis, F.; Fantacci, S.; Gratzel, M. *Inorg. Chem.* **2006**, *45*, 9245.
(3) Bolink, H. J.; Cappelli, L.; Coronado, E.; Gratzel, M.; Orti, E.; Costa, R. D.; Viruela, P. M.; Nazeeruddin, M. K. *J. Am. Chem. Soc.* **2006**, *128*, 14786.
(4) Slinker, J. D.; Gorodetsky, A. A.; Lowry, M. S.; Wang, J.; Parker, S. T.; Rohl, R.; Bernhard, S.; Malliaras, G. G. *J. Am. Chem. Soc.* **2004**, *126*, 2763.
(5) Slinker, J. D.; Bernards, D. A.; Houston, P. L.; Abruña, H. D.; Bernhard, S.; Malliaras, G. G. *Chem. Commun.* **2003**, *19*, 2392.
(6) Lowry, M. S.; Hudson, W. R., Jr.; Bernhard, S. *J. Am. Chem. Soc.* **2004**, *126*, 14129.
(7) Slinker, J. D.; Koh, C. Y.; Malliaras, G. G.; Lowry, M. S.; Bernhard, S. *Appl. Phys. Lett.* **2005**, *86*, 173506.
(8) Tamayo, A. B.; Garon, S.; Sajoto, T.; Djurovich, P. I.; Tsyba, I. M.; Bau, R.; Thompson, M. E. *Inorg. Chem.* **2005**, *44*, 8723.
(9) Lowry, M. S.; Bernhard, S. *Chem.—Eur. J.* **2006**, *12*, 7970.
(10) Su, H.-C.; Wua, C.-C.; Fang, F.-C.; Wong, K.-T. *Appl. Phys. Lett.* **2006**, *89*, 261118.
(11) Su, H.-C.; Fang, F.-C.; Hwu, T.-Y.; Hsieh, H.-H.; Chen, H.-F.; Lee, G.-H.; Peng, S.-M.; Wong, K.-T.; Wu, C.-C. *Adv. Funct. Mater.* **2007**, *17*, 1019.
(12) Slinker, J. D.; Rivnay, J.; Moskowitz, J. S.; Parker, J. B.; Bernhard, S.; Abruña, H. D.; Malliaras, G. G. *J. Mater. Chem.* **2007**, *17*, 2976.
(13) Neve, F.; LaDeda, M.; Crispini, A.; Bellusci, A.; Puntoriero, F.; Campagna, S. *Organometallics* **2004**, *23*, 5856.
(14) Lee, J. K.; Yoo, D. S.; Handy, E. S.; Rubner, M. F. *Appl. Phys. Lett.* **1996**, *69*, 1686.
(15) Maness, K. M.; Masui, H.; Wightman, R. M.; Murray, R. W. *J. Am. Chem. Soc.* **1997**, *119* (17), 3987.
(16) Handy, E. S.; Pal, A. J.; Rubner, M. F. *J. Am. Chem. Soc.* **1999**, *121*, 3525.
(17) Gao, F. G.; Bard, A. J. *J. Am. Chem. Soc.* **2000**, *122*, 7426.
(18) For a review of the science of OLEDs, see: Hung, L. S.; Chen, C. H. *Mater. Sci. Eng. Rep.* **2002**, *39*, 143.
(19) Buda, M.; Kalyuzhny, G.; Bard, A. J. *J. Am. Chem. Soc.* **2002**, *124*, 6090.
(20) Bernhard, S.; Barron, J. A.; Houston, P. L.; Abruña, H. D.; Ruglovsky, J. L.; Gao, X.; Malliaras, G. G. *J. Am. Chem. Soc.* **2002**, *124*, 13624.
(21) Rudmann, H.; Shimada, S.; Rubner, M. F. *J. Appl. Phys.* **2003**, *94*, 115.
(22) Lowry, M. S.; Goldsmith, J. I.; Slinker, J. D.; Rohl, R.; Pascal, R. A.; Malliaras, G. G.; Bernhard, S. *Chem. Mater.* **2005**, *17*, 5712.
(23) Rudmann, H.; Shimida, S.; Rubner, M. F. *J. Am. Chem. Soc.* **2002**, *124*, 4918.
(24) Nazeeruddin, M. K.; Hunmphry-Baker, R.; Berner, D.; Rivier, B. S.; Zuppiroli, L.; Grätzel, M. *J. Am. Chem. Soc.* **2003**, *125*, 8790.
(25) Slinker, J. D.; DeFranco, J. A.; Jaquith, M. J.; Silveira, W. R.; Zhong, Y.-W.; Moran-Mirabal, J. M.; Craighead, H. C.; Abruña, H. D.; Marohn, J. A.; Malliaras, G. G. *Nat. Mater.* **2007**, *6*, 894.
(26) Gorodetsky, A. A.; Parker, S. T.; Slinker, J. D.; Bernards, D. A.; Wong, M. H.; Flores-Torres, S.; Abruña, H. D.; Malliaras, G. G. *Appl. Phys. Lett.* **2004**, *84*, 807.
(27) Bernhard, S.; Gao, X.; Malliaras, G. G.; Abruña, H. D. *Adv. Mater.* **2002**, *14*, 433.
(28) Bernards, D. A.; Biegala, T.; Samuels, Z. A.; Slinker, J. D.; Malliaras, G. G.; Flores-Torres, S.; Abruña, H. D.; Rogers, J. A. *Appl. Phys. Lett.* **2004**, *84*, 3675.
(29) Bernards, D. A.; Slinker, J. D.; Malliaras, G. G.; Flores-Torres, S.; Abruña, H. D. *Appl. Phys. Lett.* **2004**, *84*, 4980.
(30) Slinker, J. D.; Rivnay, J.; DeFranco, J. A.; Bernards, D. A.; Gorodetsky, A. A.; Parker, S. T.; Cox, M. P.; Rohl, R.; Malliaras, G. G.; Flores-Torres, S.; Abruña, H. D. *J. Appl. Phys.* **2006**, *99*, 074502.
(31) Zhang, Q.; Zhou, Q.; Cheng, Y.; Wang, L.; Ma, D.; Jing, X.; Wang, F. *Adv. Funct. Mater.* **2006**, *16*, 1203.

10.1021/cm0713374 CCC: $40.75 
Published on Web 12/27/2007

and can range from seconds to hours.[5] A number of techniques have been applied to reduce turn-on time. For instance, decreasing the thickness of the iTMC layer makes the device turn-on faster; however, it also lowers its efficiency, owing to exciton quenching at the electrode.[33] Increasing the applied bias above the turn-on voltage reduces the turn-on time but also leads to shorter device lifetimes;[16,20] however, by applying a high voltage pulse and then operating the device at a lower voltage, turn-on time is reduced with minimal impact on lifetime.[16] This scheme requires more sophisticated driving electronics, and it is not compatible with all architectures and applications, such as cascaded lighting panels or direct outlet operation.[29] Thus, a viable and practical solution still must be found to overcome these limitations in devices.

Modification of either the iTMCs or their surrounding environment to promote greater ionic conductivity remains the most preferable solution to decreasing turn-on times in devices. The latter solution has been studied with moderate success. For instance, turn-on times were decreased from 2 min to 30 s with the inclusion of poly(ethylene oxide) into a film of a $Ru(phen)_3$-type complex,[34] and turn-on times were further decreased by an additional 33% with the addition of $(Li^+)(CF_3SO_3^-)$ salt. Analogously, decreased turn-on times were observed with the addition of lithium triflate/crown ether complexes into a blend containing binuclear ruthenium complexes.[35] Unfortunately, in both of these cases the external quantum efficiencies were low ($\leq$0.02%), and lifetime was reduced. Changing the nature of the counterion of the iTMCs from $PF_6^-$ to $ClO_4^-$ or $BF_4^-$ reduces the turn-on times but also is accompanied by faster degradation of the device, as observed by the decreasing light output with time.[17,19,23] More recently, a mix of a heteroleptic iridium iTMC and an ionic liquid reduced turn-on times from 5 h to 40 min, but the device lifetime was also compromised.[36]

Ionic ligands represent one way to improve turn-on time. By attaching ionic groups to the periphery, we increase the ionic conductivity. Ionic ligands have been previously used as a means to achieve novel colors in Ir electroluminescent devices. Bolink and co-workers reported the construction of a light-emitting electrochemical cell (LEEC) based on an otherwise neutral homoleptic iridium(III) complex bearing ionic tri-*n*-butylphosphonium groups appended to a ppy (ppy = 2-phenylpyridine) scaffold.[37] Blue-green electroluminescence at a peak wavelength of 487 nm was demonstrated. Herein we report utilization of ionic ligands to reduce the turn-on times of ruthenium and iridium electroluminescent devices. Namely, homoleptic ruthenium-based and heteroleptic iridium-based iTMCs were synthesized to contain tethered ionic tetraalkylammonium salts that mimic an ionic liquid.[36] Photophysical, electrochemical, and electroluminescence characteristics are presented.

## Experimental Section

**General.** Solvents and reagents were purchased from Aldrich and used without further purification. $[Ru(bpy)_3]^{2+}(PF_6^-)_2$ was prepared via a literature procedure.[38] The dimeric iridium(III) complex $[(ppy)_2Ir\text{-}\mu\text{-}Cl]_2$ was prepared in 81% yield according to the literature[6] by heating ppy-H and $IrCl_3H_2O$ in 2-ethoxyethanol to 110 °C for 15 h, followed by filtration of the yellow precipitate. $^1H$ NMR and $^{13}C$ NMR spectra were recorded on a Varian INOVA or a Brucker Avance at 500 and 125 MHz, respectively, and chemical shifts were referenced to the solvent. The following abbreviations have been used for multipilicity assignments: "s" for singlet, "d" for doublet, "t" for triplet, "m" for multiplet, and "br" for broad.

**Synthesis.** *1-Pyridylacylpyridinium Iodide (**2**).*[39] To a solution of 2-acylpyridine (**1**) (10 g, 82.5 mmol, 1 equiv) in 100 mL of pyridine was added $I_2$ (23 g, 90.8 mmol, 1.1 equiv) and heated to 100 °C under $N_2$ for 2 h. Upon cooling to room temperature (RT), the black precipitate was filtered through a Buchner funnel, copiously washed with $Et_2O$, and air-dried. The black solid was recrystallized from hot EtOH and filtered through a Buchner funnel. The solid was dried in vacuo to yield 26 g of a black crystalline solid. Yield: 97%. $^1H$ NMR (300 MHz, acetone-$d_6$): $\delta$ 9.26 (m, 2H), 8.91 (t, $J$ = 9.0 Hz, 1H), 8.85 (d, $J$ = 12.0 Hz, 1H), 8.43 (t, $J$ = 9.0 Hz, 2H), 8.11 (m, 2H), 7.82 (m, 1H), 6.81 (s, 2H).

*5-Methyl-2,2′-bipyridine (**3**).*[39] To a solution of 1-pyridylacylpyridinium iodide (**2**) (2.5 g, 7.7 mmol, 1 equiv) in 20 mL of MeOH was added methacrolein (650 $\mu$L, 7.9 mmol, 1.03 equiv) and $NH_4OAc$ (2.96 g, 38.4 mmol, 5 equiv). The solution was refluxed under $N_2$ for 20 h. Upon cooling, the reaction was quenched with $H_2O$ and extracted 5 × hexanes. The organic layer was washed 2 × $H_2O$, then dried over $MgSO_4$, and then filtered through a celite plug. The organic layer was concentrated under reduced pressure and then in vacuo to yield a light yellow liquid. Yield: 88%; $R_f$ (50% EtOAc/hexanes on alumina): 0.74. $^1H$ NMR (500 MHz, $CDCl_3$): $\delta$ 8.64 (dd, $J$ = 1.5, 4.5 Hz, 1H), 8.42 (d, $J$ = 1.5 Hz, 1H), 8.32 (d, $J$ = 8.5 Hz, 1H), 8.25 (d, $J$ = 8.5 Hz, 1H), 7.78 (dt, $J$ = 2.0, 7.5 Hz, 1H), 7.60 (dd, $J$ = 1.5, 8.5 Hz, 1H), 7.26 (ddd, $J$ = 1.5, 4.5, 7.5 Hz, 1H), 2.37 (s, 3H). $^{13}C$ NMR (125 MHz, $CDCl_3$): $\delta$ 156.3, 153.6, 149.6, 149.1, 137.5, 136.9, 133.4, 123.4, 120.8, 120.6, 18.3. EIMS $[M + Na]^+$: 193.0; EIMS $[M + H]^+$: 171.0.

*5-Bromomethyl-2,2′-bipyridine (**4a**).*[40,41] To a solution of 5-methyl-2,2′-bipyridine (**3**) (1 g, 5.9 mmol, 1 equiv) in 50 mL of $CCl_4$ was added NBS (2.3 g, 12.9 mmol, 2.2 equiv) and dibenzoyl peroxide (BPO) (142 mg, 0.6 mmol, 0.1 equiv). The solution was degassed 2× and refluxed for 2 h with constant TLC monitoring. The solution was hot vacuum filtered through a Buchner funnel and washed 3 × $CCl_4$. The solution was concentrated under reduced pressure by 2/3. The resulting white precipitate was filtered through a Buchner funnel. The precipitate was then dissolved in $CH_2Cl_2$ and concentrated. The off-white solid was purified via flash column chromatography (10% EtOAc/hexanes on alumina; $R_f$: 0.22) to yield a white solid. Yield: 30%. $R_f$ (10% EtOAc/hexanes on alumina): 0.22. $^1H$ NMR (400 MHz, $CDCl_3$): $\delta$ 8.65 (dd, $J$ = 1.2, 4.8 Hz, 2H), 8.37

(32) Howard, W. E.; Prache, O. F. *IBM J. Res. Dev.* **2001**, *45*, 115.
(33) Lee, K. W.; Slinker, J. D.; Gorodetsky, A. A.; Flores-Torres, S.; Abruña, H. D.; Houston, P. L.; Malliaras, G. G. *Phys. Chem. Chem. Phys.* **2003**, *5*, 2706.
(34) The iTMC used was tris(4,7-diphenyl-1,10-phenanthroline disulfonate)ruthenium(II): Lyons, C. H.; Abbas, E. D.; Lee, J. K.; Rubner, M. F. *J. Am. Chem. Soc.* **1998**, 12100.
(35) Leprêtre, J.-C.; Deronzier, A.; Stéphan, O. *Synth. Met.* **2002**, *131*, 175.
(36) Parker, S. T.; Slinker, J. D.; Lowry, M. S.; Cox, M. P.; Bernhard, S.; Malliaras, G. G. *Chem. Mater.* **2005**, *17*, 3187.
(37) Bolink, H. J.; Cappelli, L.; Coronado, E.; Parham, A.; Stossel, P. *Chem. Mater.* **2006**, *18*, 2778.
(38) Cooley, L. F.; Headford, C. E. L.; Elliott, C. M.; Kelley, D. F. *J. Am. Chem. Soc.* **1988**, *110*, 6673.
(39) Polin, J.; Schmohel, E.; Balzani, V. *Synthesis* **1998**, 321.
(40) Schubert, U. S.; Eschbaumer, C.; Hochwimmer, G. *Synthesis* **1999**, *5*, 779.
(41) Jimenez-Molero, M. C.; Dietrich-Buchecker, C.; Sauvage, J.-P. *Chem.—Eur. J.* **2002**, *8*, 1456.

(d, $J = 8.0$ Hz, 2H), 7.84–7.78 (m, 2H), 7.30 (dd, $J = 1.2$, 4.8, Hz, 1H), 7.29 (dd, $J = 1.2$, 4.8 Hz, 1H), 4.51 (s, 2H). $^{13}$C NMR (125 MHz, $CDCl_3$): $\delta$ 156.0, 155.5, 149.3, 149.2, 137.6, 137.0, 133.6, 123.9, 121.2, 121.0, 29.6. EIMS $[M + H]^+$: 249.0.

*5-Methyltriethylammonium-2,2′-bipyridine Bromide (**5a**).* To a solution of 5-bromomethyl-2,2′-bipyridine (**4a**) (430 mg, 1.73 mmol, 1 equiv) in 5 mL of ACN was added $NEt_3$ (1 mL). The solution was refluxed under $N_2$ for 20 h. Upon cooling, the solution was diluted with $Et_2O$. The $Et_2O$ solution was decanted, and the remaining brown oil was further copiously washed with $Et_2O$. The brown oil was dried in vacuo to yield a beige solid. Yield: 76%. $^1$H NMR (500 MHz, $CD_3CN$): $\delta$ 8.82 (d, $J = 2.0$ Hz, 1H), 8.68 (dd, $J = 2.0$, 5.0 Hz, 1H), 8.47 (d, $J = 8.0$ Hz, 1H), 8.42 (d, $J = 8.0$ Hz, 1H), 8.07 (dd, $J = 1.2$, 8.0, Hz, 1H), 7.90 (dt, $J = 1.2$, 8.0 Hz, 1H), 7.42 (ddd, $J = 1.0$, 5.0, 7.5 Hz, 1H), 4.67 (s, 2H), 3.28 (q, $J = 7.5$ Hz, 6H), 1.39 (t, $J = 7.5$ Hz, 9H). $^{13}$C NMR (125 MHz, acetone-$d_6$): $\delta$ 200.6, 158.1, 155.9, 153.7, 150.4, 142.3, 138.0, 125.5, 121.8, 121.3, 58.8, 53.9, 8.4. Anal. EIMS $[M - Br - 1]^+$: 269.0.

**General Procedure for the Synthesis of 5-Bromoalkyl-2,2′-bipyridine.** To a solution of 5-methyl-2,2′-bipyridine (1 g, 5.88 mmol, 1 equiv) in 60 mL of THF at −40 °C was added LDA (3.8 mL, 2 M, 1.2 equiv) over 5 min. The dark brown solution was allowed to stir warming from −40 to −10 °C over 1 h. This solution was added via cannula to a solution of 1,($n$ – 1)-dibromoalkane (52.9 mmol, 9 equiv) in 80 mL of THF at −40 °C. The combined mixture was allowed to stir slowly warming to RT over 18 h. The now light orange solution was quenched with $NH_4Cl$(aq) and washed with 2 × 1 M HCl. The combined aqueous fractions were back-extracted with 2 × hexanes and then neutralized with $K_2CO_3$(s). To the neutralized aqueous phase was now added $Et_2O$. The aqueous phase was further extracted with 2 × $Et_2O$. The $Et_2O$ phase was concentrated under reduced pressure and then in vacuo. The desired 5-bromoalyl-2,2′-bipyridine formed in ca. 2.5:1 with respect to 5-methyl-2,2′-bipyridine as determined by $^1$H NMR. The crude mixture was taken on to the next step without further purification.

**General Procedure for the Synthesis of 5-Alkyltriethylammonium-2,2′-bipyridine Bromide (5b–5d).** To a crude solution of a mixture of 5-bromoalkyl-2,2′-bipyridine and 5-methyl-2,2′-bipyridine in 3 mL of ACN was added $NEt_3$ (1 mL). The solution was refluxed under $N_2$ for 20 h. Upon cooling the solution was diluted with $Et_2O$. The cloudy $Et_2O$ solution was decanted, and the remaining brown oil was further copiously washed with $Et_2O$. The brown oil was dried in vacuo to yield beige-brown solids. Yield for **5b**: 28% over two steps. $^1$H NMR (500 MHz, $CD_3CN$): $\delta$ 8.64 (d, $J = 5.0$ Hz, 1H), 8.54 (d, $J = 2.0$, 1H), 8.38 (d, $J = 8.0$ Hz, 1H), 8.35 (d, $J = 8.0$ Hz, 1H), 7.87 (dt, $J = 2.0$, 8.0, Hz, 1H), 7.75 (dd, $J = 2.0$, 8.0 Hz, 1H), 7.36 (ddd, $J = 1.0$, 5.0, 7.5 Hz, 1H), 3.20 (q, $J = 7.5$ Hz, 6H), 3.12 (m, 2H), 2.76 (t, $J = 7.5$, 2H), 1.69 (m, 4H), 1.20 (tt, $J = 2.0$, 7.5 Hz, 9H). $^{13}$C NMR (125 MHz, $CD_3CN$): $\delta$ 156.6, 154.5, 150.1, 149.9, 138.4, 137.8, 137.7, 124.5, 121.1, 118.2, 57.4, 53.6, 32.2, 28.2, 21.8, 7.9. EIMS $[M - Br]^+$: 311.0. Yield for **5c**: 32% over two steps. $^1$H NMR (400 MHz, $CD_3CN$): $\delta$ 8.63 (dd, $J = 1.2$, 4.0 Hz, 1H), 8.51 (d, $J = 2.0$, 1H), 8.36 (d, $J = 8.0$ Hz, 1H), 8.32 (d, $J = 8.0$ Hz, 1H), 7.87 (dt, $J = 1.6$, 8.0, Hz, 1H), 7.72 (dd, $J = 2.4$, 8.4 Hz, 1H), 7.36 (ddd, $J = 1.2$, 4.8, 7.6 Hz, 1H), 3.18 (q, $J = 7.2$ Hz, 6H), 3.05 (m, 2H), 2.69 (t, $J = 7.6$, 2H), 1.69–1.58 (m, 4H), 1.38 (m, 4H), 1.19 (tt, $J = 1.2$, 7.2 Hz, 9H). $^{13}$C NMR (125 MHz, acetone-$d_6$): $\delta$ 157.0, 154.6, 150.2, 150.1, 139.2, 137.7, 137.6, 124.5, 121.1, 121.0, 57.8, 53.7, 33.1, 33.0, 31.6, 26.8, 22.4, 8.1. EIMS $[M - Br]^+$: 339.0. Yield for **5d**: 24% over two steps. $^1$H NMR (500 MHz, $CD_3CN$): $\delta$ 8.62 (d, $J = 4.5$ Hz, 1H), 8.50 (d, $J = 2.0$ Hz, 1H), 8.37 (d, $J = 8.0$ Hz, 1H), 8.31 (d, $J = 8.0$ Hz, 1H), 7.86 (dt, $J = 2.0$, 7.5, Hz, 1H), 7.70 (dd, $J = 2.5$, 8.5 Hz, 1H), 7.35 (ddd, $J = 1.2$, 5.0, 8.0 Hz, 1H), 3.19 (q, $J = 7.5$ Hz, 6H), 3.05 (m, 2H), 2.69 (t, $J = 7.5$, 2H), 1.65–1.58 (m, 4H), 1.38–1.28 (m, 8H), 1.19 (tt, $J = 1.5$, 7.5 Hz, 9H). $^{13}$C NMR (125 MHz, acetone-$d_6$): $\delta$ 157.4, 155.0, 150.7, 150.6, 140.0, 138.4, 138.2, 125.0, 121.7, 121.6, 58.2, 54.1, 33.6, 32.1, 30.1, 30.0, 29.9, 27.2, 22.6, 8.3. EIMS $[M - Br]^+$: 367.0.

**General Procedure for the Synthesis of Ru(bpy*)$_3$(PF$_6$)$_5$ Complexes (7a–7d).** A mixture of $RuCl_3$ (50 mg, 0.24 mmol, 1 equiv) and ligand (0.75 mmol, 3.1 equiv) were suspended in 5 mL of ethylene glycol. The mixture was microwaved for 3 × 2 min intervals (power: medium; w/200 mL of $H_2O$). After the first iteration the solution turned dark red. The solution was cooled and diluted with $H_2O$ and $NH_4Cl$(aq). The aqueous layer was successively extracted with $CH_2Cl_2$ until no more ligand was visible by TLC. The remaining $CH_2Cl_2$ was removed from the aqueous phase under reduced pressure. Black impurities present were removed by vacuum filtration. To the aqueous phase was added ca. 3 mL of 10% w/w $NH_4PF_6/H_2O$. An immediate precipitation was observed, and the mixture was placed in the freezer for 24 h. The clear supernatant was decanted, and the red precipitate was copiously washed with $H_2O$ and $Et_2O$. The precipitate was redissolved in $CH_3CN$, then concentrated under reduced pressure, and then dried in vacuo. The crude complex was recrystallized by vapor diffusion of $Et_2O$ into a $CH_3CN$ solution. Yield for **7a**: 84%. $^1$H NMR (500 MHz, $CD_3CN$): $\delta$ 8.60 (m, 6H), 8.48 (m, 6H), 8.17–8.02 (m, 12H), 7.79–7.42 (m, 15H), 4.47 (m, 6H), 4.37–4.19 (m, 6H) 3.51–3.41 (m, 9H), 3.02 (m, 18H), 1.14 (m, 27H). $^{13}$C NMR (500 MHz, $CD_3CN$): $\delta$ 157.1, 154.8, 153.3, 150.1, 143.2, 139.4, 139.3, 137.7, 129.6, 128.7, 126.6, 125.5, 73.6, 69.9, 62.1, 57.3, 54.0, 8.1. ESIMS $[M - CH_3–PF_6]^{2+}$: 673.20. ESIHRMS $[m\text{-}CH_3–PF_6]^{2+}/z$: found 673.1940; calcd ($C_{51}H_{72}F_{18}N_9P_3{}^{101}$Ru) 673.5701. Yield for **7b**: 99%. $^1$H NMR (500 MHz, acetone-$d_6$): $\delta$ 8.74–8.69 (m, 6H), 8.16 (m, 3H), 8.07 (m, 3H), 8.05–7.93 (m, 3H), 7.83–7.77 (m, 3H), 7.51 (m, 3H), 3.41 (m, 18H), 3.27 (m, 6H), 2.67 (m, 6H), 1.78 (m, 6H), 1.63 (m, 6H), 1.33 (m, 27H). $^{13}$C NMR (500 MHz, $CD_3CN$): $\delta$ 158.3, 156.2, 152.7, 152.1, 143.4, 138.9, 128.4, 125.1, 57.5, 53.9, 32.6, 27.8, 22.1, 7.9. ESIMS $[M - CH_3–PF_6]^+$: 1616.49. ESIHRMS $[m\text{-}CH_3–PF_6]^+/z$: found 1616.4932; calcd ($C_{60}H_{90}F_{24}N_9P_4{}^{101}$Ru) 1616.4929. Yield for **7c**: 99%. $^1$H NMR (500 MHz, $CD_3CN$): $\delta$ 8.49–8.42 (m, 6H), 8.04 (q, $J = 8.0$ Hz, 3H), 7.91 (t, $J = 8.0$ Hz, 3H), 7.76–7.71 (m, 3H), 7.50 (m, 3H), 7.38 (q, $J = 7.5$ Hz, 3H) 3.19 (q, $J = 7.5$ Hz, 18H), 3.04 (m, 6H), 2.52 (m, 6H), 1.54 (m, 6H), 1.44 (m, 6H), 1.22 (m, 39H). $^{13}$C NMR (500 MHz, $CD_3CN$): $\delta$ 158.2, 155.8, 152.6, 151.2, 144.1, 138.7, 128.2, 124.9, 57.8, 53.8, 32.9, 30.6, 29.1, 26.6, 22.1, 7.8. ESIMS $[M - CH_3–PF_6]^+$: 1701.59. ESIHRMS $[m\text{-}CH_3\text{-}PF_6]^+/z$: found 1701.5883; calcd ($C_{66}H_{102}F_{24}N_9P_4{}^{101}$Ru) 1701.5881. Yield for **7d**: 99%. $^1$H NMR (500 MHz, $CD_3CN$): $\delta$ 8.45–8.40 (m, 6H), 8.03 (q, $J = 8.0$ Hz, 3H), 7.88 (m, 3H), 7.68 (m, 3H), 7.45 (m, 3H), 7.36 (m, 3H), 3.17 (q, $J = 7.0$ Hz, 18H), 3.02 (m, 6H), 2.48 (m, 6H), 1.57 (m, 6H), 1.41 (m, 6H), 1.21 (m, 45H), 1.12 (m, 6H). $^{13}$C NMR (500 MHz, $CD_3CN$): $\delta$ 156.8, 156.7, 154.3, 154.2, 154.1, 151.3, 151.2, 151.1, 150.6, 150.5, 150.4, 142.8, 142.7, 142.6, 142.5, 137.4, 137.3, 137.2, 137.1, 126.8, 126.7, 123.6, 123.5, 123.4, 123.3, 56.4, 56.3, 56.2, 52.3, 52.2, 52.1, 31.6, 31.5, 29.6, 29.5, 29.4, 28.5, 28.4, 28.3, 28.2, 28.1, 25.6, 20.9, 9.3. ESIMS $[M - CH_3–PF_6]^+$: 1785.68. ESIHRMS $[m\text{-}CH_3–PF_6]^+/z$: found 1785.6790; calcd ($C_{72}H_{114}F_{24}N_9P_4{}^{101}$Ru) 1785.6820.

**General Procedure for the Synthesis of (ppy)$_2$Ir(bpy*)(PF$_6$)$_2$ Complexes (8a–8d).** A mixture of $[(ppy)_2Ir\text{-}\mu\text{-}Cl]_2$ (100 mg, 0.09 mmol, 1 equiv) and ligand (0.19 mmol, 2.1 equiv) were suspended in 3 mL of ethylene glycol and heated to 150 °C under $N_2$ for 22 h. The solution was cooled and diluted with $H_2O$ and $NH_4Cl$(aq). The aqueous layer was successively extracted with $CH_2Cl_2$ until

no more ligand was visible by TLC. The remaining $CH_2Cl_2$ was removed from the aqueous phase under reduced pressure. To the aqueous phase was added ca. 3 mL of 10% w/w $NH_4PF_6/H_2O$. An immediate precipitation was observed, and the mixture was placed in the freezer for 24 h. The clear supernatant was decanted, and the yellow precipitate was copiously washed with $H_2O$ and $Et_2O$. The precipitate was redissolved in $CH_3CN$, then concentrated under reduced pressure, and then dried in vacuo. The crude complex was recrystallized by vapor diffusion of $Et_2O$ into a $CH_3CN$ solution. Yield for **8a**: 41%. $^1$H NMR (500 MHz, acetone-$d_6$): $\delta$ 8.89 (d, $J$ = 9.0 Hz, 1H), 8.84 (d, $J$ = 8.5 Hz, 1H), 8.45 (dd, $J$ = 2.0, 8.5 Hz, 1H), 8.31 (d, $J$ = 2.0 Hz, 1H), 8.27 (dt, $J$ = 1.5, 7.5 Hz, 1H), 8.22 (t, $J$ = 8.5 Hz, 2H), 8.11 (dd, $J$ = 1.5, 5.0 Hz, 1H), 7.97–7.88 (m, 5H), 7.82 (d, $J$ = 5.5 Hz, 1H), 7.70 (dt, $J$ = 1.5, 5.5 Hz, 1H), 7.14 (m, 2H), 7.03 (m, 2H) 6.92 (m, 2H), 6.39 (d, $J$ = 7.5 Hz, 1H), 6.35 (d, $J$ = 7.5 Hz, 1H), 3.63 (ABq, $J_{AB}$ = 14.3 Hz, 2H), 3.26 (m, 6H), 1.29 (t, $J$ = 7.5 Hz, 9H). $^{13}$C NMR (500 MHz, acetone-$d_6$): $\delta$ 168.5, 168.4, 158.7, 156.0, 153.9, 151.9, 151.0, 150.6, 150.5, 150.4, 145.0, 144.9, 144.7, 140.8, 139.7, 139.6, 132.7, 132.4, 131.5, 131.3, 130.2, 129.5, 126.5, 126.1, 126.0, 125.9, 124.7, 124.5, 123.7, 123.6, 120.9, 120.8, 57.0, 53.6, 7.9. ESIMS $[M - CH_3–PF_6]^+$: 914.26. ESIHRMS $[m\text{-}CH_3–PF_6]^+/z$: found 914.2350; calcd ($C_{39}H_{40}F_6{}^{191}IrN_5P$) 914.2532. Yield for **8b**: 61%. $^1$H NMR (500 MHz, acetone-$d_6$): $\delta$ 8.77 (d, $J$ = 8.5 Hz, 1H), 8.72 (d, $J$ = 8.5 Hz, 1H), 8.23 (m, 3H), 8.15 (dd, $J$ = 2.0, 8.5 Hz, 1H), 8.07 (d, $J$ = 5.0 Hz, 1H), 7.97–7.88 (m, 5H), 7.83 (m, 2H), 7.65 (dd, $J$ = 1.0, 6.5 Hz, 1H), 7.16 (m, 2H), 7.03 (m, 2H), 6.92 (m, 2H), 6.37 (d, $J$ = 7.0 Hz, 1H), 6.34 (dd, $J$ = 7.0 Hz, 1H), 3.41 (q, $J$ = 7.5 Hz, 6H), 3.30 (t, $J$ = 8.0 Hz, 2H), 2.70 (t, $J$ = 7.5, 2H), 1.76 (m, 2H), 1.63 (m, 2H), 1.33 (t, $J$ = 7.5 Hz, 9H). $^{13}$C NMR (500 MHz, acetone-$d_6$): $\delta$ 169.1, 157.4, 155.4, 151.8, 150.6, 150.1, 145.4, 144.1, 140.9, 140.8, 140.0, 133.0, 132.9, 131.7, 129.5, 126.2, 126.0, 125.9, 125.0, 123.8, 121.2, 57.7, 54.1, 32.9, 27.8, 22.2, 8.1. ESIMS $[M - CH_3–PF_6]^+$: 956.30. ESIHRMS $[m\text{-}CH_3–PF_6]^+/z$: found 956.2996; calcd ($C_{42}H_{46}F_6{}^{191}IrN_5P$) 956.3001. Yield for **8c**: 58%. $^1$H NMR (500 MHz, acetone-$d_6$): $\delta$ 8.77 (d, $J$ = 8.5 Hz, 1H), 8.72 (d, $J$ = 8.5 Hz, 1H), 8.26 (dt, $J$ = 2.0, 8.0 Hz, 1H), 8.23 (d, $J$ = 8.0 Hz, 2H), 8.12 (dd, $J$ = 2.0, 8.5 Hz, 1H), 8.07 (d, $J$ = 5.0 Hz, 1H), 7.97 (dt, $J$ = 1.5, 5.5 Hz, 1H), 7.97 (d, $J$ = 7.5 Hz, 1H), 7.89 (m, 3H), 7.83 (m, 2H), 7.66 (ddd, $J$ = 1.0, 5.5, 7.5 Hz, 1H), 7.15 (m, 2H), 7.05 (m, 2H), 6.93 (m, 2H), 6.36 (d, $J$ = 7.5 Hz, 2H), 3.46 (q, $J$ = 7.0 Hz, 6H), 3.31 (m, 2H), 2.58 (t, $J$ = 7.5, 2H), 1.76 (m, 2H), 1.51 (m, 2H), 1.37 (tt, $J$ = 1.5, 7.0 Hz, 9H), 1.27 (m, 4H). $^{13}$C NMR (500 MHz, acetone-$d_6$): $\delta$ 168.6, 157.0, 154.6, 151.3, 150.8, 150.1, 145.0, 144.3, 140.5, 140.3, 139.6, 132.6, 132.5, 131.2, 129.0, 125.8, 125.4, 124.6, 124.5, 123.4, 120.8, 64.3, 57.6, 53.6, 32.8, 28.9, 26.6, 22.1, 7.7. ESIMS $[M - CH_3–PF_6]^+$: 984.33. ESIHRMS $[m\text{-}CH_3\text{-}PF_6]^+/z$: found 984.3319; calcd ($C_{44}H_{50}F_6{}^{191}IrN_5P$) 984.3314. Yield for **8d**: 31%. $^1$H NMR (500 MHz, acetone-$d_6$): $\delta$ 8.77 (d, $J$ = 8.5 Hz, 1H), 8.74 (d, $J$ = 8.5 Hz, 1H), 8.25 (m, 3H), 8.13 (dd, $J$ = 2.0, 8.5 Hz, 1H), 8.08 (d, $J$ = 6.0 Hz, 1H), 7.96 (t, $J$ = 7.5 Hz, 2H), 7.90 (m, 3H), 7.83 (d, $J$ = 6.5 Hz, 2H), 7.68 (t, $J$ = 6.5 Hz, 1H), 7.15 (m, 2H), 7.05 (m, 2H), 6.93 (m, 2H), 6.36 (d, $J$ = 7.0 Hz, 2H), 3.50 (q, $J$ = 7.5 Hz, 6H), 3.37 (m, 2H), 2.57 (t, $J$ = 7.5, 2H), 1.84 (m, 2H), 1.41–1.10 (m, 8H), 1.37 (tt, $J$ = 1.5, 7.0 Hz, 9H). $^{13}$C NMR (500 MHz, $CD_3CN$): $\delta$ 167.1, 167.0, 155.6, 153.1, 150.3, 150.2, 150.1, 149.8, 148.9, 148.8, 143.7, 143.6, 143.2, 138.9, 138.8, 138.2, 138.1, 131.3, 131.1, 130.1, 130.0, 127.7, 124.6, 124.5, 123.9, 123.2, 123.1, 122.2, 122.1, 119.5, 119.5, 56.4, 52.3, 31.5, 29.0, 28.3, 28.2, 27.8, 25.5, 20.8, 8.6. ESIMS $[M - CH_3–PF_6]^+$: 1012.36. ESIHRMS $[m\text{-}CH_3\text{-}PF_6]^+/z$: found 1012.3644; calcd ($C_{46}H_{54}F_6{}^{191}IrN_5P$) 1012.3627.

**Photophysical Characterization.** UV spectra were recorded at room temperature in a 1.0 cm capped quartz cuvette using a Hewlett-Packard 8453 spectrometer equipped with a diode-array detector. The samples were prepared in acetonitrile (ACN) with a concentration of 25 $\mu$M and were each degassed by bubbling a nitrogen stream saturated with ACN for 10 min. Emission spectra were recorded using a Jobin-Yvon Fluorolog-3 spectrometer equipped with double monochromators and a Hamamatsu-928 photomultiplier tube (PMT) as the detector. Right angle detection was used for the complexes, which were all excited at 400 nm. A solution of $[Ru(bpy)_3]^{2+}(PF_6^-)_2$ in ACN ($\Phi_r = 0.062$)[42] was used as the reference. The equation $\Phi_s = \Phi_r(A_r/A_s)(I_s/I_r)(n_s/n_r)^2$ was used to calculate the relative quantum yield of the sample, where $\Phi_r$ is the absolute quantum yield of the reference, $n$ is the refractive index of the solvent, $A$ is the absorbance of the reference and sample at the excitation wavelength, and $I$ is the integrated area under the corrected emission curve. The subscripts s and r refer to the sample and reference, respectively. Excited-state lifetimes were measured using the emission monochromator and PMT detector of the Jobin-Yvon Fluorolog-3 spectrometer. The samples were excited at 400 nm with an $N_2$ laser (Laser Science, Inc. VSL-337LRF, 10 ns pulse), and the emission decay was recorded using a Tektronix TDS 3032B digital phosphor oscilloscope.

**Electrochemistry.** Cyclic voltammetry were performed on a model 600C CH Instruments electrochemical analyzer. Solutions for voltammetry were prepared in acetonitrile and degassed with nitrogen bubbling for 10 min prior to scanning. Tetra(*n*-butyl)ammonium hexafluorophosphate (TBAH; 0.1 M) was used as the supporting electrolyte. A silver wire was used as the pseudo-reference electrode; a Pt wire was used for both the working and counter electrodes. The redox potentials are reported relative a saturated calomel (SCE) electrode with a ferrocenium/ferrocene ($Fc^+$/Fc) redox couple as an internal reference (0.45 V vs SCE).[43]

**Device Preparation.** All solutions were prepared and spin-cast in a nitrogen glovebox. The solutions for the pristine complex devices were made in ACN and consisted of 24 mg of complex per milliliter of solution. The films were spin-coated from solution onto glass substrates covered with prepatterned ITO electrodes. The film thicknesses were between 90 and 120 nm, as measured by profilometry. The ITO substrates were cleaned just before the deposition of the organic layer by a deionized water bath, followed by UV/ozone treatment. The films were dried for ~2 h at 120 °C on a hot plate in a dry nitrogen glovebox; thus, the films were never exposed to air. A 200 Å thick Au top electrode was deposited through a shadow mask that defined six devices per substrate with a 3 mm$^2$ active area for each. The deposition of Au was carried out intermittently to minimize heating of the organic film. The electrical characteristics of the devices were measured with a Keithley 236 source-measure unit, and the radiant flux measurements were collected with a calibrated UDT S370 optometer coupled to an integrating sphere. The electroluminescence spectra were measured with a calibrated S2000 Ocean Optics fiber spectrometer.

## Results and Discussion

**Synthesis.** The four-step synthesis of triethylammonium bromide salts (**5**) linked by an alkyl tether to a bipyridine (bpy) moiety is shown in Scheme 1. 5-Methyl-2,2′-bipyridine (5-Mebpy **3**) is formed in excellent yield from the corresponding pyridinium salt (**2**) via a Kröhnke[44] condensation. Lithiation of **3** under dilute but not optimized conditions

(42) Caspar, J. V.; Kober, E. M.; Sullivan, B. P.; Meyer, T. J. *J. Am. Chem. Soc.* **1982**, *104*, 630.
(43) Connelly, N. G.; Geiger, W. E. *Chem. Rev.* **1996**, *96*, 877.
(44) Kröhnke, F. *Synthesis* **1976**, 1.

**Scheme 1. Synthesis of Bipyridines (5) Containing a Pendant Alkyltriethylammonium Bromide[a]**

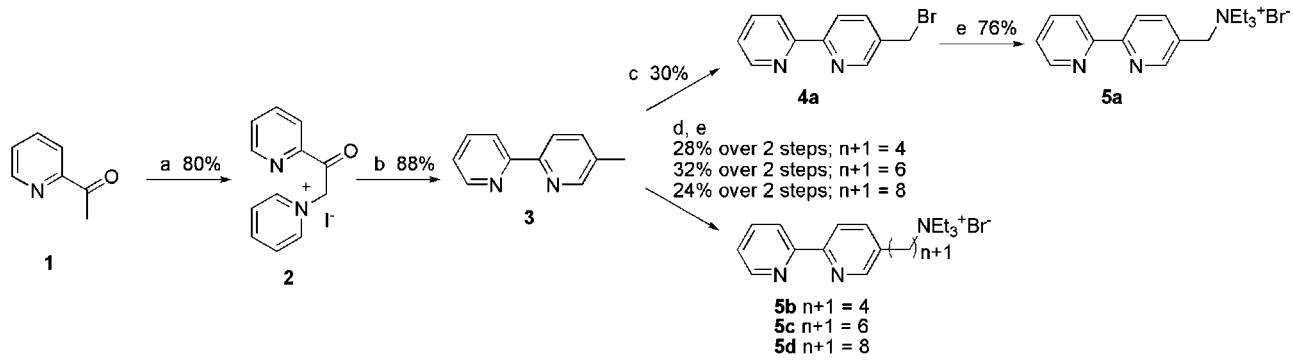


[a] Synthesis of **5**: (a) $I_2$/pyr; 80 °C, 1 h and then RT, 15 h; (b) methacrolein, $NH_4OAc$/MeOH, reflux,18 h; (c) NBS, cat. BPO/$CCl_4$, reflux, 2 h; (d) 1. LDA/THF −40 °C, 2 h. 2. 1,*n*-dibromoalkane/THF, −40 °C to RT, 15 h; (e) $NEt_3$/ACN, reflux 15 h [pyr = pyridine; NBS = *N*-bromosuccinimide; BPO = dibenzoylperoxide; LDA = lithium diisopropylamide; ACN = acetonitrile].

**Scheme 2. Synthesis of Ionic Ruthenium (7a–d) and Iridium (8a–d) Complexes Synthesis of iTMCs[a]**

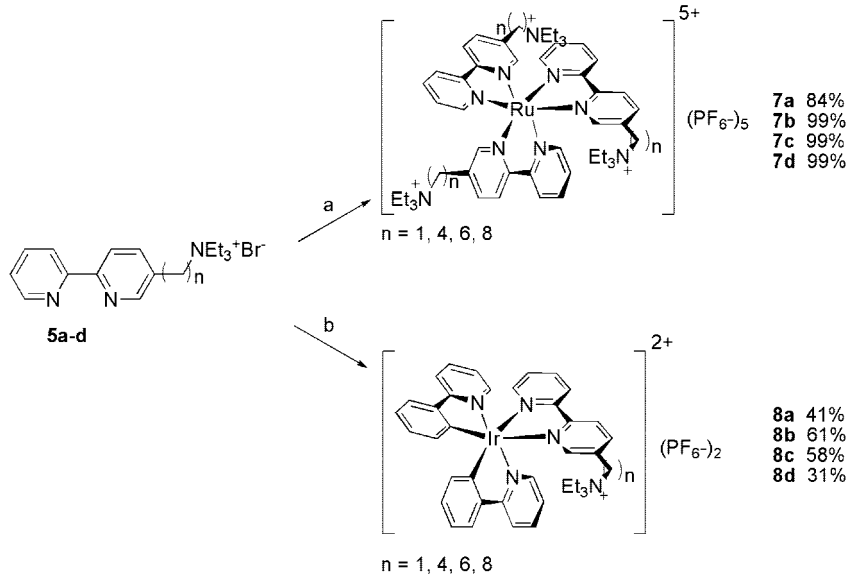


[a] Synthesis of iTMCs: (a) $RuCl_3$/EG, MW, 6 min; (b) $[(ppy)_2Ir\text{-}\mu\text{-}Cl]_2$/EG, 150 °C, 15 h [EG = ethylene glycol, MW = microwave].

followed by quenching with excess 1,*n*-dibromoalkane resulted in a ca. 2.5:1 mixture of desired bromoalkylbpy to starting material as determined by $^1$H NMR. This crude mixture was reacted with $NEt_3$ in refluxing ACN, with the ammonium salt either precipitating or filming out of solution upon addition of $Et_2O$ after cooling. In this manner, a 4-carbon (**5b**), a 6-carbon (**5c**) and an 8-carbon (**5d**) tether were synthesized in moderate yield over the two steps. Radical monobromination of **3** afforded **4a** in moderate yield. Upon treatment of **4a** with $NEt_3$, the one-carbon congener (**5a**) was formed in good yield.

With the suitably functionalized bipyridines in hand, metal complexation occurred readily (Scheme 2) to afford a series of homoleptic ruthenium tris(bpy*) complexes (**7a–d**) and a corresponding series of heteroleptic $(ppy)_2Ir$(bpy*) complexes (**8a–d**) (bpy* = **5a–d**). Ruthenium complexes were efficiently formed by treatment of $RuCl_3$ with 3 equiv of diimine ligand in the microwave. Iridium complexes were formed by cleaving the bridging chlorides of the corresponding iridium dimer with the bpy* ligands (**5a–d**). All complexes were isolated as their $PF_6^-$ salt through anion metathesis using $NH_4PF_6$ and were recrystallized by vapor diffusion of diethyl ether into a saturated acetonitrile solution.

**Photophysical and Electrochemical Properties.** The absorption and emission data of all the complexes are summarized in Table 1. Figure 1 shows the absorption spectra of the complexes in ACN at room temperature. All the ruthenium complexes exhibit a characteristic strong band at around 290 nm that is assigned to a ligand-centered (LC) singlet $^1(\pi\rightarrow\pi^*)$ transition localized on the bipyridine ligand, with complexes **7a–d** slightly bathochromically shifted relative to $[Ru(bpy)_3]^{2+}$. Weaker bands observed in the visible region are indicative of a $^1$MLCT (d$\rightarrow\pi^*$) transition with a small bathochromic shift and plateauing observed for

**Table 1. Absorption and Luminescence Data of All the Ruthenium and Iridium Complexes[a,b]**

| | absorption | room temperature emission | | | | |
|---|---|---|---|---|---|---|
| compound | $\lambda_{max}$, nm ($\epsilon$, $10^3$ $M^{-1}$ $cm^{-1}$) | $\lambda_{max}$, nm | $\tau$, $\mu$s | $\Phi^c$ | $k_r$ ($10^5$ $s^{-1}$) | $k_{nr}$ ($10^5$ $s^{-1}$) |
| $Ru(bpy)_3$ | 287 (109.3), 451 (22.3) | 605 | 1.10 | 0.06 | 0.6 | 8.5 |
| **7a** | 292 (113.5), 453 (20.1) | 630 | 0.89 | 0.03 | 0.3 | 10.9 |
| **7b** | 293 (101.4), 448 (17.2) | 606 | 0.84 | 0.05 | 0.6 | 11.4 |
| **7c** | 292 (101.2), 448 (17.1) | 604 | 0.71 | 0.05 | 0.7 | 13.4 |
| **7d** | 291 (4.8), 449 (4.0) | 602 | 0.78 | 0.05 | 0.6 | 12.3 |
| **8a** | 254 (4.7), 315 (4.4), 366 (3.9) | 619 | 0.09 | 0.01 | 0.8 | 110.3 |
| **8b** | 255 (4.9), 315 (4.6), 369 (4.1) | 576 | 0.71 | 0.13 | 1.9 | 12.1 |
| **8c** | 255 (4.8), 315 (4.4), 364 (3.8) | 568 | 0.74 | 0.21 | 2.8 | 10.7 |
| **8d** | 256 (4.5), 312 (4.2), 364 (3.6) | 572 | 0.50 | 0.09 | 1.8 | 18.4 |

[a] Measured in nitrogen-saturated acetonitrile solvent. [b] $\epsilon$, $\varphi$, and $\tau$ are $\pm$10% or better. [c] The emission quantum yields were measured vs $[Ru(bpy)_3](PF_6)_2$ – $\lambda_{ex}$ = 400 nm.

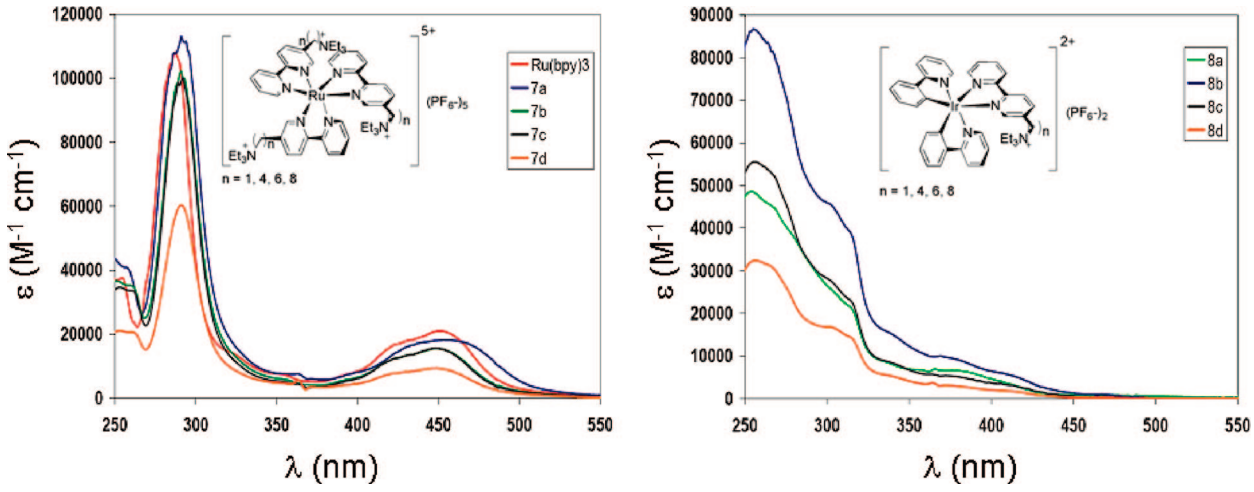


**Figure 1.** Absorption spectra of the complexes in nitrogen-saturated 25 $\mu$M acetonitrile solutions.

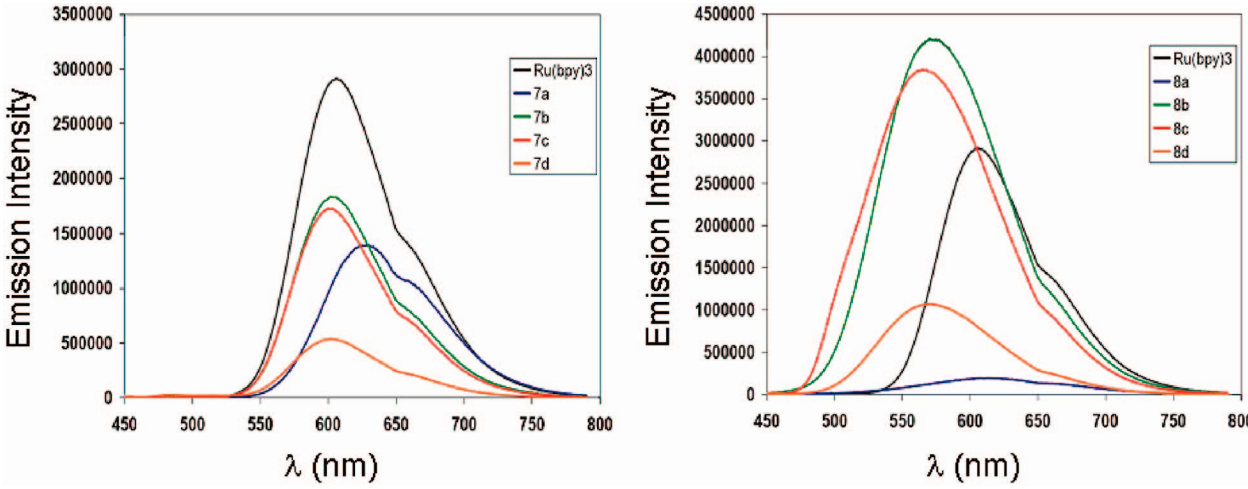


**Figure 2.** Uncorrected room temperature emission spectra of the complexes in nitrogen-saturated 25 $\mu$M acetonitrile solutions ($\lambda_{ex}$ = 400 nm).

**7a** for this absorption band. The absorption spectra for the iridium analogues (**8a–d**) are unremarkable as compared to other phenylpyridine-type heteroleptic iridium complexes with the presence of $\pi$–$\pi$* LC bands at $\lambda$ < 300 nm and absorption features at $\lambda$ > 300 nm attributed mainly to $^1$MLCT transitions.[45] Clearly, the alkyltriethylammonium substituents do not significantly perturb the absorbance spectrum.

The emission spectra are shown in Figure 2. All the complexes exhibit broad and undistinguished emissions characteristic of combined $^3$MLCT and $^3\pi$–$\pi$* LC transitions as assigned by Güdel for similar complexes.[46,47] Iridium complexes exhibited RT $\Phi_{em}$ 2–4 times that of the analogous ruthenium materials. Unlike the absorption spectra, the emission spectra exhibit marked differences when the alkyl tether is shortened to a single methylene group. A characteristic bathochromic shift of ca. 30 nm is observed for the ruthenium complex **7a**; a larger bathochromic shift of 50 nm is observed for the iridium analogue, **8a**. These batho-

(45) Schmid, B.; Garces, F. O.; Watts, R. J. *Inorg. Chem.* **1994**, *33*, 9.
(46) Colombo, M. G.; Guedel, H. U. *Inorg. Chem.* **1993**, *32*, 3081.
(47) Colombo, M. G.; Hauser, A.; Guedel, H. U. *Inorg. Chem.* **1993**, *32*, 3088.

**Table 2. Redox Properties of Selected Ruthenium and Iridium Complexes[a,b]**

| compound[a,b] | $E°$ $M^{n+}/M^{(n+1)b}$ (V vs SCE) | $\Delta E_p$ (mV) | $E°$ $L/L^-$ (V vs SCE) | $\Delta E_p$ (mV) |
|---|---|---|---|---|
| $Ru(bpy)_3$ | +1.26 | 70 | −1.36 | 58 |
| **7a** | +1.43 | 153 | −1.03 | c |
| **7c** | +1.28 | 100 | −1.44 | 88 |
| **8a** | +1.38 | 89 | −1.01 | c |
| **8c** | +1.26 | 110 | −1.48 | 84 |

[a] Cyclic voltammetry was carried out at 100 mV/s in 0.1 M TBAH/$CH_3CN$ at a Pt working electrode with a Pt counter electrode and an Ag wire as a pseudo-reference. Ferrocene was used as an internal standard, and potentials are reported with respect to a saturated calomel (SCE) electrode. [b] For ruthenium complexes, $n = 2$; for iridium complexes, $n = 3$. [c] Irreversible wave.

chromic shifts result from the large inductive effect imparted by the triethylammonium group. A decrease in the emission lifetime coupled with a dramatic drop in quantum efficiency (from ca. 14% in **8b–d** to 1% for **8a**) is indicative of adherence to the energy gap law in these complexes. Complexes with longer alkyl chains exhibit excited-state characteristics similar to their parent compounds: Ruthenium complexes **7b–d** resemble $Ru(bpy)^{2+}$ while iridium complexes **8b–d** resemble $[(ppy)_2Ir(5,5'\text{-dmbpy})]^+$ ($\lambda_{em} = 558$ nm, $\Phi = 0.20$, $\tau = 0.9$ $\mu$s; 5,5′-dmbpy = 5,5′-dimethyl-2,2′-bipyridine) and $[(ppy)_2Ir(dtb\text{-}bpy)]^+$ ($\lambda_{em} = 570$ nm, $\Phi = 0.18$, $\tau = 0.5$ $\mu$s; dtb-bpy = 4,4′-di-*tert*-butyl-2,2′-bipyridine) but with a small (ca. 12 nm) bathochromic shift compared to the former control complex.[6] The difference in solution photoluminescence quantum yields for the series **8b–d** can be rationalized by their relative intermolecular spacing, a trend that is also observed in the solid state (vide infra).

The cyclic voltammetry data for a subset of the complexes are summarized in Table 2 and show reversible oxidation waves of the metals. Given that the complexes bearing longer chains (**7b–d**, **8b–d**) exhibit similar photophysical behavior, we used **7c** and **8c** as representative complexes for the series during our electrochemical investigations. Compared to the oxidation waves of **7c** and **8c**, those of **7a** and **8a** are anodically shifted by 150 and 120 mV, respectively, because of the inductive electron-withdrawing nature of the triethylammonium group. The ligand-based first reduction potential, which corresponds to the energy of the LUMO, is significantly anodically shifted for both **7a** and **8a** as compared to **7c** and **8c**, respectively. Thus, though the triethylammonium group in **7a** and **8a** stabilizes both the metal-based HOMO and the ligand-based LUMO, the stabilization of the LUMO is more significant, resulting in an overall decrease in the HOMO–LUMO gap, a property that is also observed in the red-shifted emission spectra and further demonstrates that the energy gap law applies. The reduction waves for **7a** and **8a** are irreversible owing to facile hemolytic cleavage of the C–N bond to form a stabilized benzylic radical and triethylamine. Not surprisingly, the CV data for **7c** closely mirror that of $Ru(bpy)_3^{2+}$ while that of **8c** resembles that of $[(ppy)_2Ir(bpy)]$.[48]

**Device Characteristics.** *Ruthenium Complexes.* In Figure 3 we show the radiant flux versus time for ITO/[Ru complex]/Au devices operating at 3 V. Those based on compounds **7b** and **7c** yield dramatically improved turn-on times. The times for onset of emission ($t_{on}$), defined as the time to achieve emission above 20 nW, are 12 and 4 s, respectively, as compared to about 1 min for the $[Ru(bpy)_3]^{2+}(PF_6^-)_2$ device. Likewise, the time to maximum radiant flux $t_{max}$ is reduced from over 15 min for $[Ru(bpy)_3]^{2+}(PF_6^-)_2$ to 3 and 1 min for **7b** and **7c**, respectively. This improvement suggests that the alkyltriethylammonium ligands of **7b** and **7c** are efficient transporters of ionic charges. The turn-on time was also reduced by the **7d** compound, but to a lesser extent. **7d** yielded a $t_{on}$ and $t_{max}$ of 42 and 145 s, respectively. The turn-on time was not improved by the **7a** compound. The poor electrochemical stability of **7a** under reduction (vide infra) and the low quantum yield indicate that this compound is likely an inferior electron transporter and a poor emitter, leading to a low efficiency, a long turn-on time, and a short lifetime in the device.

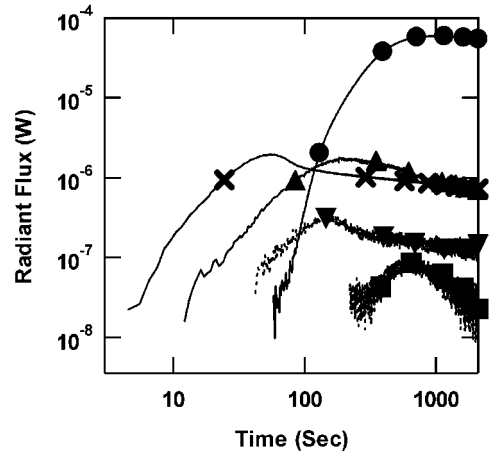


**Figure 3.** Log radiant flux vs log time for ITO/[Ru complex]/Au devices. The curves are labeled as follows: **7a**, squares (■); **7b**, upward triangles (▲); **7c**, crosses (×); **7d**, downward trianges (▼); $[Ru(bpy)_3]^{2+}(PF_6^-)_2$, circles (●).

The **7b–d** compounds show relatively good lifetimes. In Figure 4 we show the current and radiant flux versus time for **7b**, **7c**, **7d**, and $[Ru(bpy)_3]^{2+}(PF_6^-)_2$ devices. Radiant flux half-lives $t_{1/2}$ of 63, 87, and 66 min are attained for the steady-state operation of **7b–d**, respectively, comparable to the 142 min value of $[Ru(bpy)_3]^{2+}(PF_6^-)_2$ devices. However, it can be seen that both the current and radiant flux are substantially lower for **7b–d** complexes, lowering monotonically with increasing side chain length. The maximum luminance from devices **7b–d** are 72, 66, and <10 cd/m$^2$, respectively. This could indicate that the bulky alkyltriethylammonium ligands are increasing the average spacing between the complexes such that electronic charge transport is encumbered. This drop in the magnitude of the luminance of the **7b–d** devices without an increase in lifetime has negative implications for

(48) Goldsmith, J. I.; Hudson, W. R.; Lowry, M. S.; Anderson, T. H.; Bernhard, S. *J. Am. Chem. Soc.* **2005**, *127*, 7502.

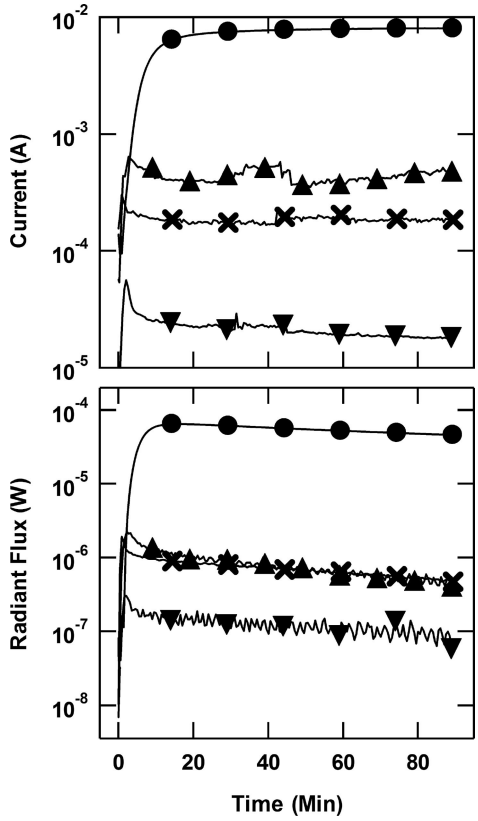


**Figure 4.** Radiant flux vs time for ITO/[Ru complex]/Au devices. The curves are labled as follows: **7b**, upward triangles (▲); **7c**, crosses (×); **7d**, downward triangles (▼); $[Ru(bpy)_3]^{2+}(PF_6^-)_2$, circles (●).

**Table 3. Turn-On Time, Efficiency, Half-Life, and Electroluminescence Spectral Data for 3 V Operation of ITO/[Ru Complex]/Au Devices**[a]

| compound | $t_{on}$ (s) | $t_{max}$ (min) | $\eta_{max}$ (%) | $t_{1/2}$ (min) | $\lambda_{max}$ (nm) |
|---|---|---|---|---|---|
| $Ru(bpy)_3^{2+}$ | 58 | 16.5 | 0.68 | 142 | 615 |
| **7a** | 221 | 9.3 | 0.01 | 11 | 612 |
| **7b** | 12 | 3.1 | 0.17 | 63 | 599 |
| **7c** | 5 | 0.9 | 0.43 | 87 | 599 |
| **7d** | 42 | 2.4 | 0.27 | 66 | 605 |

[a] Spectral data were collected at 4 V.

chromophore stability.[12] Nonetheless, the maximum external quantum efficiencies $\eta_{max}$ for **7b–d** are respectable and are similar to the trends in the photoluminescence quantum yields, demonstrating that the electronic charge balance is minimally affected relative to $[Ru(bpy)_3]^{2+}(PF_6^-)_2$. ITO and Au electrodes have previously been shown to be ohmic for hole and electron injection in $[Ru(bpy)_3]^{2+}(PF_6^-)_2$ devices,[26] suggesting that the exciton formation efficiency is still close to 1 for these materials. The values of $\eta_{max}$, along with the turn-on time, lifetime, and electroluminescence data, are presented in Table 3.

*Iridium Complexes.* Likewise, alkyltriethylammonium side chains can improve the turn-on times of Ir electroluminescent devices. In this case, we compared the performance of complexes **8a**, **8b**, and **8c** with the iridium complex $[(ppy)_2Ir(dtb\text{-}bpy)]^+(PF_6^-)$, where dtb-bpy is 4,4′-di-*tert*-butylbipyridine. This complex has been shown to yield devices with $\eta_{max}$ as high as 5% but having long turn-on times on the order of hours.[4] Results for the **8d** complex are not presented as this material did not produce

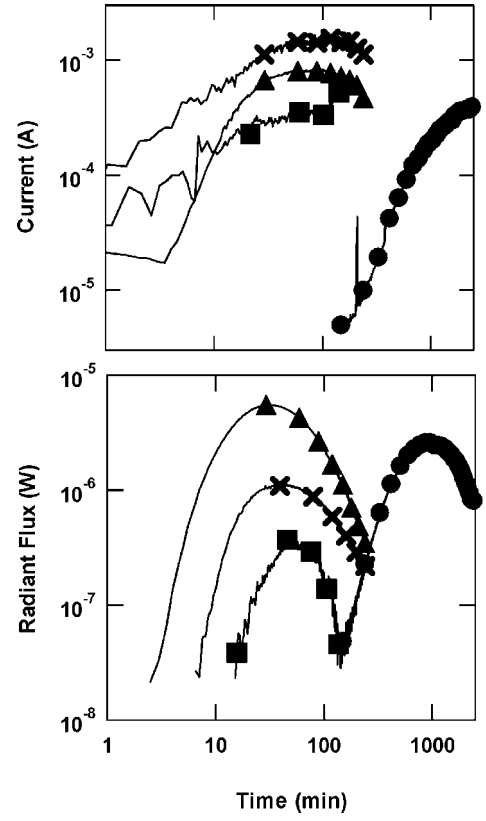


**Figure 5.** Log current and radiant flux vs log time for ITO/[Ir complex]/Au devices. The curves are labeled as follows: **8a**, squares (■); **8b**, triangles (▲); **8c**, crosses (×); $[(ppy)_2Ir(dtb\text{-}bpy)]^+(PF_6^-)$, circles (●).

**Table 4. Turn-On Time, Efficiency, Half-Life, and Electroluminescence Spectral Data for −3 V Operation of ITO/[Ir Complex]/Au Devices**[a]

| compound | $t_{on}$ (min) | $t_{max}$ (min) | $\eta_{max}$ (%) | $t_{1/2}$ (min) | $\lambda_{max}$ (nm) |
|---|---|---|---|---|---|
| $(ppy)_2Ir(dtb\text{-}bpy)^+$ | 140 | 940 | 1.75[49] | 988 | 573 |
| **8a** | 15 | 33 | 0.06 | 57 | 595 |
| **8b** | 2.5 | 33 | 0.71 | 54 | 569 |
| **8c** | 7 | 38 | 0.05 | 87 | 568 |
| **8d** | n/a | n/a | n/a | n/a | n/a |

[a] Spectral data were collected at –6 V.

device-quality films, yielding only shorted devices. A log–log plot of radiant flux vs time data is shown for ITO/[Ir complex]/Au devices is presented in Figure 5, while the corresponding values of $\eta_{max}$, $t_{on}$, $t_{max}$, $t_{1/2}$, and $\lambda_{max}$ are presented in Table 4. In this case, the $[(ppy)_2Ir(dtb\text{-}bpy)]^+(PF_6^-)$ devices take over 100 min to initiate emission and do not reach saturation until nearly 1000 min into operation. Devices based on the **8a–c** complexes show dramatically improved $t_{on}$ values of 15, 2.5, and 7 min, respectively. Likewise, $t_{max}$ is reduced by over an order of magnitude to 33, 33, and 38 min for **8a–c**, respectively. Thus, the ionic ligands can reduce the turn-on time of Ir-based iTMC devices by nearly 2 orders of magnitude. Interestingly, these turn-on times are comparable to that found in the $[Ru(bpy)_3]^{2+}(PF_6^-)_2$ device, which carries the same charge density per metal center ($2e$). Also, in comparison, adding ionic liquids in a 0.5 molar ratio with $[(ppy)_2Ir(dtb\text{-}bpy)]^+(PF_6^-)$ reduced $t_{on}$ and $t_{max}$ to 6 and 40 min, respectively.[36] The radiant flux

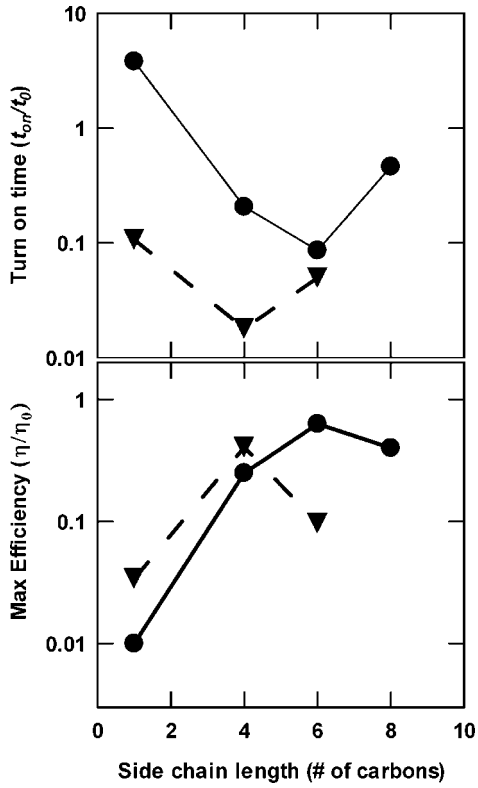


**Figure 6.** Normalized turn-on time and maximum external quantum efficiency vs alkylammonium side chain length (in number of carbons) for ruthenium and iridium complexes. Ruthenium data are noted by solid lines and circles (●) and iridium data by dashed lines and triangles (▼). The lines are guides to the eye. Ruthenium data were normalized against $[Ru(bpy)_3]^{2+}(PF_6^-)_2$, while iridium complexes were normalized against $[(ppy)_2Ir(dtb\text{-}bpy)]^+(PF_6^-)$.

maximum of **8b** is comparable to that obtained for $[(ppy)_2Ir(dtb\text{-}bpy)]^+(PF_6^-)$, achieving a maximum luminance of 300 cd/m$^2$. The steady-state currents of the **8a–c** compounds were all greater than or equal to that for $[(ppy)_2Ir(dtb\text{-}bpy)]^+(PF_6^-)$. This implies that the intermolecular spacings of the complexes are comparable, a plausible assertion given the bulky nature of the dtb-bpy ligand. Also, in comparison with the Ru data, the relative radiant fluxes of the Ir complexes are enhanced by having only one modified ligand. The external quantum efficiency values for **8a** and **8b** follow the photoluminescence quantum yield trends relative to $[(ppy)_2Ir(dtb\text{-}bpy)]^+(PF_6^-)$ (for which $\Phi = 0.18$[6]), suggesting balanced electronic injection is achieved. However, **8c** significantly departs from this trend, having a significantly lower $\eta_{ext}$ than would be expected from the quantum yield data, implying a loss of electron and hole carrier balance in the device. As was the case for the **7a** (ruthenium) complex, the **8a** complex showed lower radiant flux and external quantum efficiency as anticipated from the poor electrochemical stability under reduction and the lower quantum yield. The half-lives of **8b** and **8c** (54 and 87 min) are comparable to those obtained for the ruthenium analogues but lower than the pristine complex, which is on the order of tens of hours.[36] It has previously been postulated[36] that increasing the ionic conductivity can negatively impact the lifetime of Ir electroluminescent devices due to irreversible multiple oxidation of the complexes;[48] multiple oxidation is reversible for $[Ru(bpy)_3]^{2+}(PF_6^-)_2$ complexes. We are currently investigating the fundamental degradation modes of Ir complexes.

We summarize the results for the alkyltriethylammonium-modified ruthenium and iridium complexes in Figure 6. The data are normalized to $[(ppy)_2Ir(dtb\text{-}bpy)]^+(PF_6^-)$ for the iridium complexes and $[Ru(bpy)_3]^{2+}(PF_6^-)_2$ for the ruthenium materials. The turn-on time is greatly reduced for all iridium complexes, while it is reduced for ruthenium analogues with side chain lengths of 4, 6, and 8 carbons. For both metal centers, device efficiency is improved in extending the carbon chain length from 1 to 4 methylenes due to improved electrochemical stability under reduction and improved photoluminescence efficiency. The initial rise in quantum efficiency correlates with the PL quantum yield and electrochemical stability results. The subsequent drop in efficiency with chain length for the six-carbon **8c** analogue is attributed to nonoptimal spacing of the phosphorescent metal centers, which impedes electronic transport. Optimal $t_{on}$ and $\eta_{ext}$ are found with the four-carbon side chain iridium complex (**8b**) and with the six-carbon side chain (**7c**) ruthenium complexes.

*Applicability.* In principle, the incorporation of tetraalkylammonium groups can endow any transition metal complex with high ionic conductivity, within the constraints of electrochemical stability noted above. This holds true even for neutral complexes—in this manner a TMC can be turned into an iTMC to endow them with ionic conductivity. This can in turn provide compatibility with air-stable electrodes[26,27] and ac driving techniques.

## Conclusions

We have reported the facile fabrication of a series of iridium and ruthenium and iridium iTMCs possessing pendant triethylammonium groups. The presence of these ionic moieties dramatically shortens the turn-on times of the devices. Optimal device characteristics were found when the chain length separation between the bipyridine ligand and the triethylammonium group was found to be six methylene units for ruthenium and four methylene units for iridium. To our knowledge, these are the fastest turn-on times for pristine heteroleptic iridium complexes.

**Acknowledgment.** This work was supported by the New York State Office of Science, Technology and Academic Research (NYSTAR), by the National Science Foundation (DMR-0605621 and CAREER Award No. CHE-0449755 (S.B.)), and through a Camille and Henry Dreyfus Foundation New Faculty Award (S.B.). E.Z.-C. acknowledges support from PCCM in the form of a postdoctoral fellowship scholarship. J.D.S. was supported by a National Science Foundation Graduate Research Fellowship.

CM0713374

(49) This value is lower than that obtained previously in ref 4. The devices presented in this work were thicker than those prepared previously, and the films were baked on a hot plate in a nitrogen glovebox (as opposed to a vacuum oven) to avoid exposure of the films to air. These steps were taken in order to minimize variations in turn-on time due to fluctuations in the thickness or humidity and instead emphasize intrinsic materials properties.